

Synthesis, Crystal Structure, and Thermal Behavior of the Rare Earth Sulfates $(\text{H}_5\text{O}_2)\text{M}(\text{SO}_4)_2$ ($\text{M} = \text{Ho}, \text{Er}, \text{Y}$)

Mathias S. Wickleder*

Institut für Anorganische Chemie, Universität zu Köln Greinstrasse 6, D-50939 Köln, Germany

Received April 22, 1998. Revised Manuscript Received June 26, 1998

The compounds $(\text{H}_5\text{O}_2)\text{M}(\text{SO}_4)_2$ ($\text{M} = \text{Ho}, \text{Er}, \text{Y}$) were obtained from the metal oxides M_2O_3 ($\text{M} = \text{Ho}, \text{Er}, \text{Y}$) using diluted sulfuric acid (80%). The crystal structure of the isotypic compounds has been determined from single-crystal data by direct and Fourier methods [tetragonal, $I4_1/amd$ (No. 141); $(\text{H}_5\text{O}_2)\text{Ho}(\text{SO}_4)_2$, $a = 6.9140(5)$ Å, $c = 17.246(2)$ Å, $R = 0.013$; $(\text{H}_5\text{O}_2)\text{Er}(\text{SO}_4)_2$, $a = 6.8967(7)$ Å, $c = 17.166(2)$ Å, $R = 0.012$; $(\text{H}_5\text{O}_2)\text{Y}(\text{SO}_4)_2$, $a = 6.8875(7)$ Å, $c = 17.159(2)$ Å, $R = 0.016$]. The characteristic feature of the crystal structure is a network of edge-sharing $[\text{MO}_8]$ trigon dodecahedra and $[\text{SO}_4]$ tetrahedra providing channels along $[111]$ which are occupied by disordered H_5O_2^+ ions. In situ X-ray powder investigations exhibit that the compounds are also formed as intermediate phases during the reaction of the hydrogen sulfates $\text{M}(\text{HSO}_4)_3$ ($\text{M} = \text{Ho}, \text{Er}, \text{Y}$) with water. According to DSC measurements and temperature-dependent powder diffraction studies, the thermal decomposition of the title compounds follows a two-step mechanism. Around 150 °C, two molecules of water are driven off, yielding $\text{M}(\text{HSO}_4)(\text{SO}_4)$ ($\text{M} = \text{Ho}, \text{Er}, \text{Y}$), and finally, at 320 °C, H_2SO_4 ($\text{H}_2\text{O} + \text{SO}_3$) is released to give the anhydrous sulfates $\text{M}_2(\text{SO}_4)_3$.

Introduction

Sulfates of the rare earth elements and their derivatives have rarely been investigated. Reliable structural data are available only for a few compounds, namely hydrates such as $\text{Pr}(\text{SO}_4)_2 \cdot 8\text{H}_2\text{O}$ and "ternary" sulfates such as $\text{NaNd}(\text{SO}_4)_2$.^{1–3} Recently, the hydrogen sulfates of some rare earth elements, $\text{M}(\text{HSO}_4)_3$ ($\text{M} = \text{La}, \text{Ce} - \text{Er}$) were synthesized by the reaction of lanthanide oxides with concentrated sulfuric acid at elevated temperatures.^{4–5} Reduction of the acid concentration and the reaction temperature then led to the oxonium rare earth sulfate hydrates $(\text{H}_5\text{O}_2)\text{M}(\text{SO}_4)_2$. There is one compound of the same composition described in the literature ($\text{M} = \text{Ce}$),⁶ but its structure is found to be completely different. Two further oxonium compounds, $\text{H}_3\text{OLa}(\text{SO}_4)_2 \cdot 3\text{H}_2\text{O}$ and $(\text{H}_3\text{O})_3\text{Nd}(\text{SO}_4)_3 \cdot \text{H}_2\text{O}$, are available under similar conditions and will be discussed elsewhere.⁷ In this study, the crystal structure of the title compounds and their thermal behavior will be presented. Furthermore, it is shown that the compounds are intermediate products during the hydration of the respective hydrogen sulfates.

Experimental Section

Single crystals of the compounds $(\text{H}_5\text{O}_2)\text{M}(\text{SO}_4)_2$ ($\text{M} = \text{Ho}, \text{Er}, \text{Y}$) were grown as follows: 1 g of the oxides Ho_2O_3 (99.99%,

Aldrich), Y_2O_3 (99.99%, Aldrich), and Er_2O_3 (99.99%, Heraeus), respectively, was dissolved in 30 mL of hot (100 °C) sulfuric acid (Merck p.a, concentrated 80% H_2SO_4). After cooling, the solutions were allowed to stand in closed vessels for 5 days. During this time, crystals of orange-yellow $(\text{H}_5\text{O}_2)\text{Ho}(\text{SO}_4)_2$, pink $(\text{H}_5\text{O}_2)\text{Er}(\text{SO}_4)_2$, and colorless $(\text{H}_5\text{O}_2)\text{Y}(\text{SO}_4)_2$ grew as elongated octahedra up to a size of 5 mm. The crystals were washed with absolute tetrahydrofuran free of their mother liquor. Due to their moisture sensitivity, the crystals must be handled in an argon filled glovebox. Small crystals of about 0.1 mm in diameter were prepared in glass capillaries for X-ray data collection. The scattering intensities were collected with an imaging plate diffractometer (STOE&CIE). The systematic absences in the collected data set led to the tetragonal space group $I4_1/amd$ (No. 141) for the three compounds. Structure solution and refinement were carried out using the programs SHELXS86 and SHELXL93.⁸ A numerical absorption correction was applied after optimization of the crystal shape (programs X-RED and X-SHAPE⁹). The data collection parameters and the determined crystallographic data are given in Tables 1–3.

DSC/TG investigations were performed using a STA 409 thermal analyzer (NETZSCH). For that purpose, about 10 mg of the substances was placed in corundum containers and heated at a constant rate of 10 K/min under flowing argon. The thermal decomposition was followed from 30 °C up to 500 °C. For the DSC data, a baseline correction was applied. Characteristical points such as the start and end temperatures

* The author may be contacted by Fax (0221 470 5083) or e-mail (mathias.wickleder@uni-koeln.de).

(1) (a) Sherry, G. J. *Solid State Chem.* **1976**, *19*, 271. (b) Larsson, L. O.; Linderbrandt, S.; Niinistö, L.; Skoglund, O. *Suomen Kemistilehti B* **1973**, *76*, 314. (c) Hiltunen, L.; Niinistö, L. *Cryst. Struct. Commun.* **1976**, *5*, 561.

(2) (a) Sirotinkin, S. P.; Tchijov, S. M.; Prokovskii, A. N.; Kovba, L. M. *J. Less-Common Met.* **1987**, *58*, 101. (b) Sirotinkin, S. P.; Prokovskii, A. N.; Kovba, L. M. *Sov. Phy. Crystallogr.* **1981**, *26*, 219.

(3) (a) Lindgren, O. *Acta Chem. Scand.* **1977**, *A31*, 591. (b) Blackburn, A. C.; Gerkin, R. E. *Acta Crystallogr.* **1994**, *C50*, 835.

(4) (a) Wickleder, M. S. *Z. Anorg. Allg. Chem.* **1998**, *624*, 1347. (b) Hummel, H. U.; Joeg, P.; Pezzeri, G.; Wolski, A. *Z. Naturforsch.* **1994**, *49b*, 347.

(5) Wickleder, M. S. *Z. Anorg. Allg. Chem.* **1998**, *624*, in press.

(6) Gatehouse, B. M.; Pring, A. *J. Solid State Chem.* **1981**, *38*, 116.

(7) Wickleder, M. S., to be published.

(8) Sheldrick, G. M., *SHELXS86 and SHELXL93: Programs for solution and refinement of crystal structures*; University of Göttingen: Göttingen, 1986/1993.

(9) (a) Fa. STOE & Cie, *X-RED 1.07: Data Reduction for STADIA and IPDS*, Darmstadt, 1996. (b) Fa. STOE & Cie, *X-SHAPE 1.01: Crystal Optimisation for Numerical Absorption Correction*, Darmstadt, 1996.

Table 1. Data Collection Parameters and Crystal Data for $(\text{H}_5\text{O}_2)\text{M}(\text{SO}_4)_2$; M = Ho (1), Er (2), Y (3)

	1	2	3
lattice parameters (Å)	$a = 6.9140(5)$ $c = 17.246(2)$	$a = 6.8967(7)$ $c = 17.166(2)$	$a = 6.8875(7)$ $c = 17.159(2)$
molar volume (cm^3/mol)	124.1	122.9	122.6
no. of formula units, Z	4		
crystal system	tetragonal		
space group	$I4_1/amd$ (No. 141)		
diffractometer	STOE IPDS		
radiation	Mo $K\alpha$ (graphite monochromator, $\lambda = 0.7107 \text{ \AA}$)		
temperature ($^\circ\text{C}$)	20		
data range	$6^\circ < 2\theta < 48^\circ$	$6^\circ < 2\theta < 48^\circ$	$6^\circ < 2\theta < 48^\circ$
index range	$-9 \leq h \leq 9$ $-8 \leq k \leq 9$ $-21 \leq l \leq 22$	$-9 \leq h \leq 9$ $-9 \leq k \leq 9$ $-20 \leq l \leq 22$	$-7 \leq h \leq 7$ $-7 \leq k \leq 7$ $-19 \leq l \leq 19$
rotation angle range;	$0^\circ < \varphi < 200^\circ$;	$0^\circ < \varphi < 200^\circ$;	$0^\circ < \varphi < 200^\circ$;
φ -increment	$\Delta\varphi = 2^\circ$	$\Delta\varphi = 1.5^\circ$	$\Delta\varphi = 2^\circ$
no. of images	100	133	100
exposure time	2.5 min	4.0 min	4.0 min
detector distance	60 mm	60 mm	80 mm
data corrections	polarization/Lorentz		
absorption corrections	numerical, after crystal shape optimization ⁹		
μ (cm^{-1})	101.4	108.2	97.3
no. of collected reflections	2364	2387	2374
no. of unique reflections	189	188	190
no. of reflections with $I_0 > 2\sigma(I)$	188	186	176
R_{int}	0.0320	0.0301	0.0464
structure determination	SHELXS-86 and SHELXL-93 ⁸		
scattering factors	International Tables, Vol. C ¹⁷		
goodness of fit	1.063	1.042	1.088
R_1 ; wR_2 $I_0 > 2\sigma(I)$	0.0135;	0.0122;	0.0156;
	0.0351	0.0353	0.0360
R_1 ; wR_2 (all data)	0.0137;	0.0126;	0.0166;
	0.0352	0.0356	0.0365

of the thermal effects were taken from the differentiated DSC curve following common procedures.¹⁰

Temperature-dependent powder diffraction data were collected using a powder diffractometer (STOE&CIE) equipped with a position sensitive detector and a graphite furnace. The fine powdered samples were prepared in silica capillaries (i.d. = 0.3 mm) and sealed with grease (APIEZON L) for protection against moisture. Data were collected in Debye-Scherrer geometry in the range of $2\theta = 7^\circ$ – 60° at temperatures of 30, 60, 120, 180, 240, 300, and 360 $^\circ\text{C}$, respectively. After each heating period, the system was allowed to equilibrate for 30 min. The data were processed by applying smoothing and background corrections using the program package VISUAL X-POW¹¹ (STOE&CIE). The same program allowed for lattice parameter refinements based on least-squares procedures.

The reaction of hydrogen sulfates $\text{M}(\text{HSO}_4)_3$ (M = Ho, Er, Y), which were synthesized following the route given in ref 4, with water (moisture), was investigated on a θ/θ powder diffractometer (STOE&CIE) equipped with a HDK 2.4 reaction chamber (BÜHLER). Powder samples were placed on a small silver plate in the chamber, which was first purged with dry N_2 . After collection of the first diffractogram, a small window of the chamber was opened to allow moisture to enter. Eight diagrams were continuously collected in the range $2\theta = 7^\circ$ – 60° . The data were handled using the program VISUAL X-POW.

(10) Hemminger, W. F.; Cammenga, H. K. *Methoden der Thermischen Analyse*; Springer Verlag: New York, 1989.

(11) Fa. STOE & Cie, *Visual X-Pow: Software package for Stoe Powder Diffraction Systems*, Darmstadt, 1996.

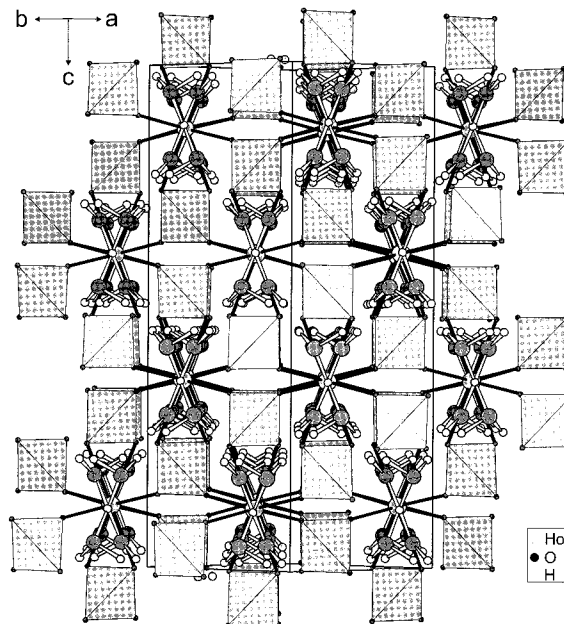


Figure 1. Crystal structure for $(\text{H}_5\text{O}_2)\text{Ho}(\text{SO}_4)_2$ viewed along $[110]$; $[\text{SO}_4]^{2-}$ groups are drawn as polyhedra; Ho–O bonds are black; both orientations of the H_5O_2^+ ion are shown.

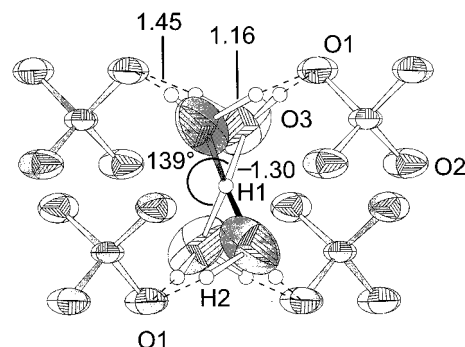


Figure 2. The H_5O_2^+ ion in $(\text{H}_5\text{O}_2)\text{Ho}(\text{SO}_4)_2$: The O3 position is only half-occupied, the resulting orientations of the ion are shown as dark gray and light gray O3 atoms and O3–H1 bonds, respectively; hydrogen bridging is indicated by broken lines, distances are given in Å.

Results and Discussion

Crystal Structure.¹⁸ The compounds $(\text{H}_5\text{O}_2)\text{M}(\text{SO}_4)_2$ (M = Ho, Er, Y) crystallize in a hitherto unknown structure type with the tetragonal space group $I4_1/amd$. The crystallographic data are given in Tables 1 and 2. The structure consists of $[\text{MO}_8]$ polyhedra which can be grasped as trigon dodecahedra. These are connected to six sulfate groups in two different ways: Along $[001]$, two $[\text{SO}_4]$ groups are attached via two common edges, and in the (001) plane, linkage occurs to four additional $[\text{SO}_4]$ groups via vertexes (Figure 1). Thereby each sulfate group belongs to three M^{3+} ions and the connectivity can be written as $\text{M}(\text{SO}_4)_{6/3} = \text{M}(\text{SO}_4)_2$ following Niggli's notation. H_5O_2^+ ions are incorporated in the three-dimensional framework of these polyhedra. This leads to an alternating occupancy of dodecahedral voids with M^{3+} and H_5O_2^+ , respectively, along $[110]$ (Figure 1). The H_5O_2^+ ions are disordered in the way depicted in Figure 2. Free refinement of the site occupation factor of the oxygen atom O3 clearly revealed an occupancy of 0.5 of this position (16h, Table 2).

Table 2. Positional Parameters and Equivalent Isotropic Displacement Parameters for (H₅O₂)M(SO₄)₂ (M = Ho in italics, M = Y bold type)

atom	site	<i>x/a</i>	<i>y/b</i>	<i>z/c</i>	<i>U</i> _{eq} · 10 ⁻¹ , pm ² ^a
Er	4a	0	3/4	1/8	10.5(2)
<i>Ho</i>	<i>0</i>	<i>0</i>	<i>3/4</i>	<i>1/8</i>	<i>10.9(2)</i>
Y	0	0	3/4	1/8	13.4(2)
S	8e	0	1/4	0.9482(1)	12.7(4)
	<i>0</i>	<i>0</i>	<i>1/4</i>	<i>0.94814(9)</i>	<i>12.8(3)</i>
	0	0	1/4	0.94830(5)	14.7(2)
O1	16h	0	0.0823(5)	0.7522(2)	22.9(4)
	<i>0</i>	<i>0</i>	<i>0.0832(5)</i>	<i>0.7516(1)</i>	<i>20.8(7)</i>
	0	0	0.0824(3)	0.7518(1)	22.9(4)
O2	16h	0	0.5780(5)	0.8992(2)	24.5(4)
	<i>0</i>	<i>0</i>	<i>0.5781(5)</i>	<i>0.8991(2)</i>	<i>22.1(7)</i>
	0	0	0.5779(3)	0.8994(1)	24.5(4)
O3 ^b	16h	0	0.1551(16)	0.4402(6)	51.2(24)
	<i>0</i>	<i>0</i>	<i>0.1584(16)</i>	<i>0.4406(6)</i>	<i>47.9(24)</i>
	0	0	0.1569(9)	0.4400(3)	54.2(16)
H1	4b	0	1/4	3/8	108(88) ^c
	<i>0</i>	<i>0</i>	<i>1/4</i>	<i>3/8</i>	<i>53(48)^c</i>
	0	0	1/4	3/8	99(39)^c
H2 ^b	32i	0.624(19)	0.715(18)	0.977(7)	150(91) ^c
	<i>0.64(2)</i>	<i>0.70(4)</i>	<i>0.970(8)</i>	<i>147(87)^c</i>	
	0.608(7)	0.684(8)	0.963(3)	57(20)^c	

^a $U_{eq} = 1/3[U_{11} + U_{22} + U_{33}]$.¹² ^b Site half-occupied. ^c Isotropic displacement parameter.

Table 3. Selected Internuclear Distances [Å] and Angles [deg] for the Compounds (H₅O₂)M(SO₄)₂ (M = Er, Ho, Y)

	M = Er	M = Ho	M = Y
M–O2 (4×)	2.300(3)	2.306(3)	2.297(2)
M–O1 (4×)	2.404(3)	2.420(3)	2.408(2)
S–O2 (2×)	1.454(3)	1.458(3)	1.452(2)
S–O1 (2×)	1.482(3)	1.477(3)	1.476(2)
O1–S–O1	102.6(3)	102.6(3)	102.9(1)
O1–S–O2 (4×)	111.20(8)	111.24(9)	111.09(6)
O2–S–O2	109.3(3)	109.1(3)	109.4(1)
Hydrogen Bonding			
O3–H2	1.13	1.17	0.85
O3–H1	1.29	1.30	1.287
H2–O1	1.51	1.45	1.74
O3–O1	2.608(5)	2.610(4)	2.603(3)
O3–O3	2.475(3)	2.436(3)	2.410(3)
O3–H2–O1	162.9	172.8	174.8
O3–H1–O3	137.3	139.6	138.8

Furthermore, complete occupation would lead to O3–O3 distances of 1.3 Å. Two orientations of the H₅O₂⁺ ion are possible, leading to short O3–O1 distances of about 2.6 Å, yielding effective hydrogen bonding between H2 and O1 (Table 3). Due to the disorder, the displacement parameters of O3 are quite large. From X-ray data, however, one cannot decide whether one deals with a dynamic process or a static order/disorder phenomenon. Another interesting feature of the H₅O₂⁺ ion is the position of the atom H1. From inspection of the difference Fourier map, the most likely location is 0, 1/4, 3/8. As can be seen from Figures 1 and 2, respectively, this leads to a symmetric O3–H1–O3 hydrogen bond. A strong argument for such an arrangement is the short O3–O3 distance of 2.44 Å within the ion. It compares well with systems such as H₂SO₄·4H₂O¹³ (2.43 Å) or HClO₄·2H₂O¹⁴ (2.42 Å), where a symmetric hydrogen bond or at least a low barrier double minimum potential has been assumed. In contrast to these

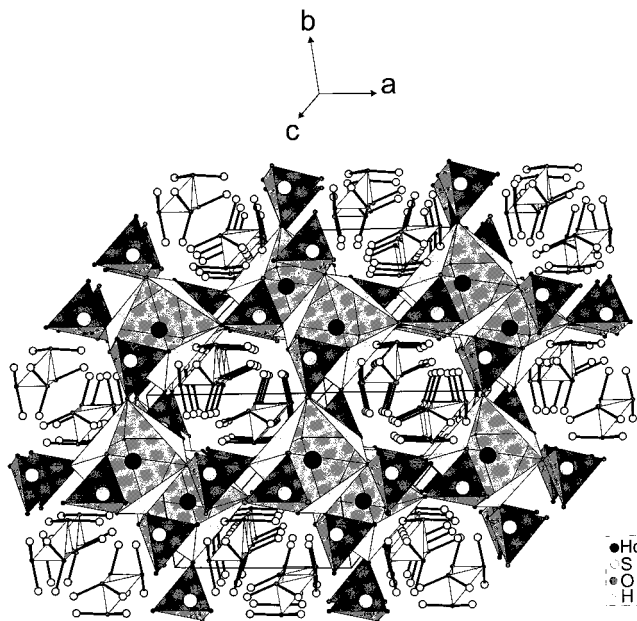


Figure 3. Crystal structure of (H₅O₂)Ho(SO₄)₂ viewed along [111]: All possible O3 positions are drawn and connected to distorted tetrahedra centered by H1. These tetrahedra are localized in channels running down this direction; O3–H2 bonds are emphasized in black.

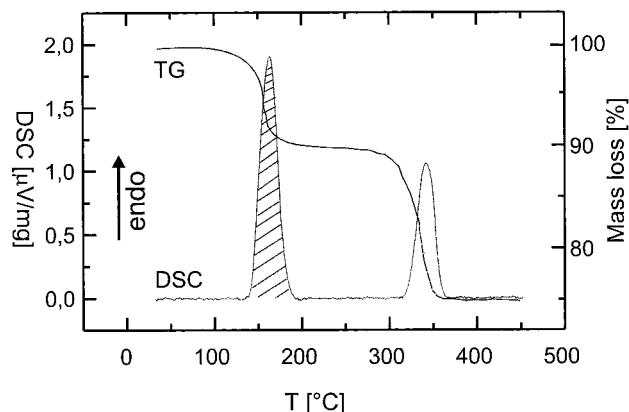


Figure 4. DSC investigation of the thermal decomposition of (H₅O₂)Y(SO₄)₂: The baseline-corrected DSC curve shows two endothermic effects at 163 and 342 °C. Both effects are correlated with a mass loss indicated by the TG curve.

systems, however, where the bond angle O–H–O is near 180°, the compounds under investigation show an O3–H1–O3 angle of 140° (Table 3), which indicates a nonsymmetric hydrogen bond. This, however, cannot be judged with certainty from the X-ray investigations. Assuming the given H1 and all possible O3 positions, the H₅O₂⁺ (=H(H₂O)₄) ions can be drawn as elongated tetrahedra. These are arranged in channels along [111] with the nearest O–O distances of 2.92 Å bearing the possibility of protonic motion along this direction (Figure 3).

Thermal Behavior. By thermal treatment the compounds (H₅O₂)M(SO₄)₂ (M = Ho, Er, Y) decompose in a two-step mechanism that is discussed in detail for the yttrium compound in the following text. The DSC measurement (Figure 4) shows a mass loss of 10.4% in the range of 147–172 °C and a second mass loss of 14.9% in the range of 333–352 °C (Table 4). The first step can be assigned to the loss of two molecules of water

(12) Fischer, R. X.; Tillmanns, E. *Acta Crystallogr.* **1988**, *C44*, 775.

(13) Kjällman, Th.; Olovsson, I. *Acta Crystallogr.* **1972**, *B28*, 1692.

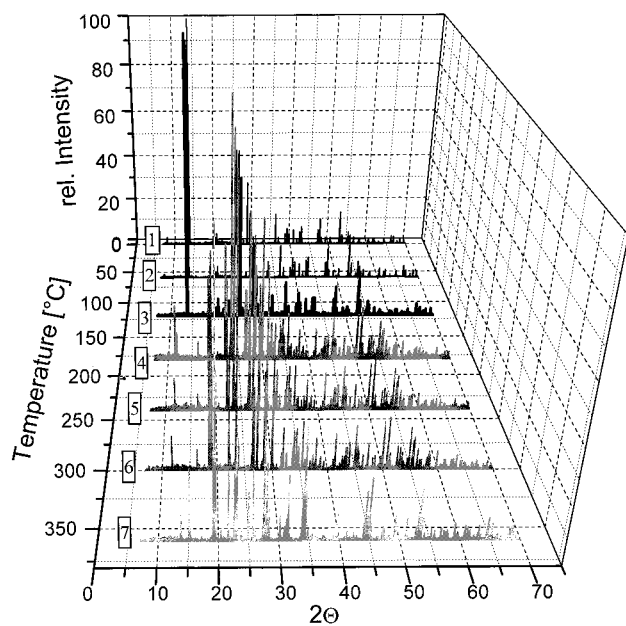
(14) Olovsson, I. *J. Chem. Phys.* **1968**, *3*, 1063.

Table 4. DSC Results of the Thermal Decomposition of (H₅O₂)Y(SO₄)₂

reaction	<i>T</i> _{start} (°C)	<i>T</i> _{end} (°C)	<i>T</i> _{max} (°C)	mass loss	
				obsd	calcd
(H ₅ O ₂)Y(SO ₄) ₂ $\xrightarrow{-2\text{H}_2\text{O}}$ Y(HSO ₄) ₂ (SO ₄)	147.4	172.4	163.5	10.2	11.3
Y(HSO ₄) ₂ (SO ₄) ₂ $\xrightarrow{-1/2\text{H}_2\text{SO}_4}$ 1/2Y ₂ (SO ₄) ₃	333.3	351.8	341.9	14.9	15.4
				Σ = 25.1	Σ = 26.7

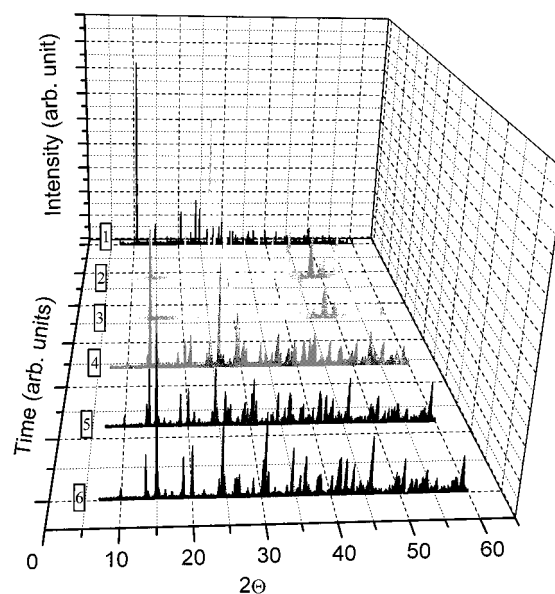
Table 5. X-ray Powder Diffraction Results of the Thermal Decomposition of (H₅O₂)Y(SO₄)₂

<i>T</i> , °C	compound	space group	<i>a</i> , Å	<i>b</i> , Å	<i>c</i> , Å	β, deg	<i>V</i> _m , cm ³ /mol
30	(H ₅ O ₂)Y(SO ₄) ₂	<i>I</i> A ₁ / <i>amd</i>	6.8549(3)		17.278(1)		122.21
60	(H ₅ O ₂)Y(SO ₄) ₂	<i>I</i> A ₁ / <i>amd</i>	6.8502(3)		17.285(1)		122.19
120	(H ₅ O ₂)Y(SO ₄) ₂	<i>I</i> A ₁ / <i>amd</i>	6.8831(6)		17.258(2)		123.12
180	Y(HSO ₄) ₂ (SO ₄)	<i>P</i> 2 ₁ / <i>n</i>	5.4970(3)	10.8001(8)	10.6023(7)	104.307(6)	91.84
240	Y(HSO ₄) ₂ (SO ₄)	<i>P</i> 2 ₁ / <i>n</i>	5.4967(3)	10.8045(5)	10.6126(6)	104.288(6)	91.97
300	Y(HSO ₄) ₂ (SO ₄)	<i>P</i> 2 ₁ / <i>n</i>	5.4968(4)	10.8088(6)	10.6244(5)	104.291(6)	92.11
360	Y ₂ (SO ₄) ₃	<i>P</i> <i>bcn</i>	12.767(1)	9.1315(8)	9.2286(6)		162.01

**Figure 5.** Temperature-dependent X-ray powder diffraction of (H₅O₂)Y(SO₄)₂: The diagrams 1 and 2 belong to (H₅O₂)Y(SO₄)₂, diagram 3 is mainly the same, but a few peaks of Y(HSO₄)₂(SO₄) start to occur. Up to 300 °C, the diffraction patterns (4–6, gray) can be assigned to Y(HSO₄)₂(SO₄). At 360 °C, Y₂(SO₄)₃ has formed (7, light gray).

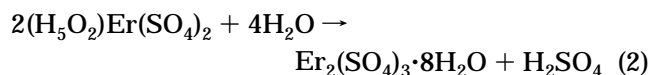
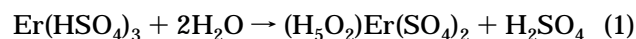
(calcd 11.3%) and the second step corresponds to the loss of 0.5 mol of sulfuric acid (calcd 15.4%). The decomposition reactions and the related data are given in Table 4.

The suggested mechanism is supported by temperature-dependent powder diffraction investigations (Figure 5). At 30 and 60 °C, the diffractograms could be indexed using simulated patterns based on single-crystal data. The same is true for the measurement at 120 °C, although a few reflections between 2θ = 18–30° remained unindexed. The unindexed reflections can be assigned to Y(HSO₄)₂(SO₄), which begins to form at this temperature. The difference in the decomposition temperatures determined by DSC and powder diffraction can be attributed to the different measuring conditions of the two methods. At 180 °C, the diffractogram contains only reflections of Y(HSO₄)₂(SO₄). Indexing was possible using single-crystal data of Er(HSO₄)₂(SO₄) which were obtained recently.⁴ Y(HSO₄)₂(SO₄) remains stable at 300 °C, but complete decomposition to Y₂(SO₄)₃

**Figure 6.** X-ray powder investigation of the hydration of Er(HSO₄)₃ (pattern 1, black): In the first step, (H₅O₂)Er(SO₄)₂ formed rapidly (patterns 2 and 3, light gray). Further hydration yields Er₂(SO₄)₃·8H₂O (patterns 5 and 6, black). In diffractogram 4 (gray) (H₅O₂)Er(SO₄)₂ and Er₂(SO₄)₃·8H₂O occur simultaneously.

is observed at 360 °C. The powder diffractogram of the latter compound could be indexed using the single-crystal data of Er₂(SO₄)₃.⁴ The refined lattice parameters of all compounds are given in Table 5.

Hydration of M(HSO₄)₃ (M = Ho, Er, Y). The first step of the reaction of hydrogen sulfates M(HSO₄)₃ (M = Ho, Er, Y) with H₂O leads to the title compounds (H₅O₂)M(SO₄)₂ (M = Ho, Er, Y) and, finally, to the formation of the octahydrates M₂(SO₄)₃·8H₂O. This is shown in Figure 6 for M = Er. The diffraction patterns collected during the reaction could be indexed using the single-crystal data of Er(HSO₄)₃,⁴ Er₂(SO₄)₃·8H₂O,¹⁵ and (H₅O₂)Er(SO₄)₂. The reaction sequence is given by the equations:



Both reactions are typical acid/base reactions with H₂O

Table 6. X-ray Powder Diffraction Results for the Hydration of Er(HSO₄)₃

no.	compound	space group	<i>a</i> , Å	<i>b</i> , Å	<i>c</i> , Å	β, deg	<i>V_m</i> , cm ³ /mol
1	Er(HSO ₄) ₃	<i>Pbca</i>	11.976(1)	9.503(1)	16.467(2)		141.11
2	(H ₅ O ₂)Er(SO ₄) ₂	<i>I4₁/amd</i>	6.878(1)		17.139(4)		122.09
3	(H ₅ O ₂)Y(SO ₄) ₂	<i>I4₁/amd</i>	6.876(2)		17.141(4)		122.03
4	(H ₅ O ₂)Y(SO ₄) ₂	<i>I4₁/amd</i>	6.864(5)	6.646(6)	17.159(9)	101.95(7)	121.73
	Er ₂ (SO ₄) ₃ •8H ₂ O	<i>C2/c</i>	13.432(6)		18.161(8)		238.14
5	Er ₂ (SO ₄) ₃ •8H ₂ O	<i>C2/c</i>	13.446(5)	6.657(4)	18.173(6)	101.98(3)	239.60
6	Er ₂ (SO ₄) ₃ •8H ₂ O	<i>C2/c</i>	13.438(4)	6.640(3)	18.184(5)	101.97(4)	238.12

acting as the base. In reaction 1, the HSO₄⁻ ion plays the role of the acid, and in reaction 2, it is the H₅O₂⁺ ion. It is noteworthy that no formation of Er(HSO₄)₃•H₂O¹⁶ is observed during the first reaction, and the compound Er₂(SO₄)₃•4H₂O¹⁶ is not observed. The conversion of Er(HSO₄)₃ seems to occur quite rapidly, while the formation of the octahydrate takes some time, as

can be seen from the fourth diffractogram (Figure 6, Table 6), where both compounds occur together.

Acknowledgment. I am indebted to Prof. Dr. G. Meyer for his generous support.

CM980301W

(15) Wickleder, M. S., to be published.

(16) Wickleder, M. S., to be published.

(17) Hahn, Th. (Ed.) *International Tables for Crystallography*; D. Reidel Publishing Company: Dordrecht, 1983; Vol. A.

(18) Crystallographic data are available from the Fachinformationszentrum Karlsruhe, D-76344 Eggenstein-Leopoldshafen (crysdata@FIZ-Karlsruhe.de) by giving the deposition numbers CSD 408876 (H₅O₂-Ho(SO₄)₂), CSD 408875 (H₅O₂Er(SO₄)₂), and CSD 408877 (H₅O₂Y(SO₄)₂), respectively.